ARKIV FÖR FYSIK Band 18 nr 21

Communicated 25 May 1960 by Bengt Edlén and Torsten Gustafsson

Photoprotons from fluorine

By B. Forkman and I. Wahlström

With 8 figures in the text

SUMMARY

The results of a study of the (γ, p) reaction in F^{19} are presented. Thin foils of teflon have been irradiated with bremsstrahlung of 15.5 and 19 MeV maximum energy. The photoprotons were recorded by nuclear emulsions. Each irradiation gives a proton spectrum containing well-resolved peaks. The peaks in the low-energy spectrum correspond to transitions from excited states in F^{19} to the ground state in O^{18}. The information about these transitions has then been used to analyze the high-energy spectrum. In this way it has been possible to interpret the proton spectrum at the high-energy irradiation as transitions from resonances in F^{19} to the ground state and excited states in O^{18}. The observed fine structure in the (γ, p) absorption has been compared with measurements of (γ, n); the agreement is found to be quite satisfactory. The angular distribution of the protons has been measured and gives further information about the photon-absorption process.

Introduction

A number of papers have treated the photodisintegration of fluorine below and within the giant resonance (γ, n) [1–6] and (γ, p) [7]. The (γ, n) investigations show that the shape of the giant resonance is considerably broader than usual. Most of the experiments show a fine structure in the absorption process, which indicates that the photons are absorbed in narrow resonances. This fine structure appears as breaks in the photoneutron activation curve or the neutron-yield curve and as peaks in the energy distribution of photoneutrons measured by time of flight technique; or by photoprotons recorded in nuclear emulsions. The first method needs quite a good energy stabilization of the accelerator. The energy value of the observed resonances will then be determined with great accuracy. It is often difficult, however, to analyze breaks in the activation curve or neutron-yield curve, especially if the curve is steep. It is thus difficult for different laboratories to obtain identical results. The method of determining the energies and the angular distribution of the emitted photoparticles gives not only information about the energy value of the resonances but also about the nature of the photo-absorption. It may be difficult, however, to interpret the energy spectrum when the nucleus is excited so strongly that it can be de-excited even to excited levels in the daughter nucleus. The spectrum can, however, be interpreted if it is compared with the spectrum from an irradiation at such a low maximum bremsstrahlung energy that the excited mother nucleus is only de-excited to the ground state in the daughter nucleus.

The aim of this work is to study the (γ, p) process in the lower part of the nuclear photoresonance in F^{19}, and to compare the results obtained with the above-mentioned (γ, n) and (γ, p) measurements. It is also desirable to find out how the F^{19} nucleus decays to various levels in the daughter nucleus O^{18}. Finally the angular distribution of the protons gives information about the spin and parity of the levels involved and thus further information about the nature of the photon absorption.

The present study is the third in a series of investigations devoted to the light nuclei being carried out in Lund. The first one concerned the photodisintegration of oxygen [8, 9] and the second the photoprotons from nitrogen [10].

Experimental arrangement

Exposures

In this experiment the photons were obtained from the bremsstrahlung beam of the 30 MeV synchrotron of the University of Lund. The beam was collimated with lead to give a pencil with a diameter of 2 cm at the position of the fluorine target. As a target a 15-μ-thick teflon foil was used. The area was 5.0 × 5.0 cm^2. The target was fixed on an inset, which fitted a cylindrical camera (Fig. 1). The inset as well as the inside of the camera were covered with lead. The teflon foil was fixed so that the angle between its normal and the photon beam was 83°.

The photoprotons were recorded in Ilford C2 nuclear emulsions, 200 μ or 400 μ thick according to the irradiation energies. The nuclear-emulsion plates were glued to shelves fixed obliquely in the inset so that the surface plane of the plates coincided with a tangent plane of the γ-beam. The innermost edge of the plates was 0.7 cm from the tangent line. The position of the camera in relation to the γ-beam has been described in our work on photoprotons from nitrogen [10]. As in the case of irradiation of nitrogen the protons had to pass a paraffin layer and a cadmium sheet to suppress the neutron flux. The target was irradiated at the 15.5 and 19 MeV maximum bremsstrahlung energies. At each energy two kinds of irradiations were carried out, a main irradiation and an irradiation with a blind lead collimator to find out the background effect of the neutrons. In addition an irradiation was made without the teflon foil but with an open collimator to determine possible photoprotons from the camera walls. To determine the angular distribution of the photoprotons yet another irradiation at the 15.5 MeV maximum bremsstrahlung energy was made with a teflon target with an area of 1.5 × 5.0 cm^2 and a thickness of 50 μ. The total dose amounted to about 500 roentgen at each one of these irradiations.

Measurements

After processing, the plates were scanned in a room in which the humidity was 65 %. The horizontal and vertical projections of the lengths of the proton tracks were measured, as well as the angle between the horizontal projection and the γ-beam. After the shrinkage factor had been determined the range of the tracks in the emulsion was calculated. The energy of the photoprotons was obtained from Barkas' range-energy tables [11]. The angle between the proton track and the γ-beam direction was calculated from the length and angle measurements.

In order to determine the energy of the proton at the ejection, it is necessary to consider the energy loss in the teflon target. The chemical composition of teflon is

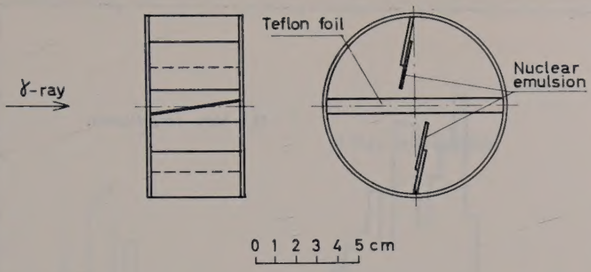

Fig. 1. Experimental arrangement of the teflon target and the nuclear emulsion plates.

C_nF_{n+2}. To determine the stopping power of the teflon we have used Bethe's formula [12] with I_0 (Bloch's const.) $= I/Z = 12.4$ eV. Since it is impossible to decide where in the teflon foil the reaction takes place we have corrected to the middle of the foil. From the background irradiations with blind collimator an isotropic distribution of the proton tracks in the nuclear emulsions was obtained. This distribution is low-energetic and arises partly from (n, p) reactions in the emulsions or from recoil protons, when neutrons collide with hydrogen nuclei in the emulsion, partly from (n, p) reactions in the surrounding matter. In those cases when protons have started in the emulsion and passed the surface, they can be mistaken for tracks of the opposite direction. One ought, however, to be able to distinguish them, since they do not have a characteristic track-end, but the separation is hard to perform, since they are low-energy tracks.

The background irradiations made without the teflon target showed that the photoprotons from other materials can be quite neglected. As the background was found to be isotropic, it can thus as well be estimated by measuring tracks in the main plates in angle sections where the tracks cannot be derived from reactions in the teflon target. In the main plates we thus measured, on the one hand, tracks that came from the teflon target, and, on the other hand, tracks that were found in the same angle sections, but instead were directed towards the γ-beam. These background tracks were corrected in the same way as those from the teflon target.

Only tracks longer than 25 μ were measured. By doing this the background from α-tracks became negligible.

Results

The photoprotons obtained from the two main irradiations at 15.5 and 19 MeV group themselves around discrete energy values. Fig. 2 shows the distribution of protons from the teflon target obtained at the 15.5 MeV irradiation. In order to obtain a good energy resolution those photoprotons that had ranges in the teflon foil longer than 30 μ have been excluded on account of the excessive correction. In the same figure the background tracks are also shown. The background as regards size and energy distribution is similar to the background that was obtained for irradiations of oxygen and nitrogen [9, 10] performed in Lund earlier. Its effect on the results in this experiment is unimportant.

The distribution of protons after subtracting the background is shown in Fig. 3. Fig. 4 shows the corresponding proton distribution obtained at the 19 MeV irradiation. Both energy spectra show well-resolved peaks.

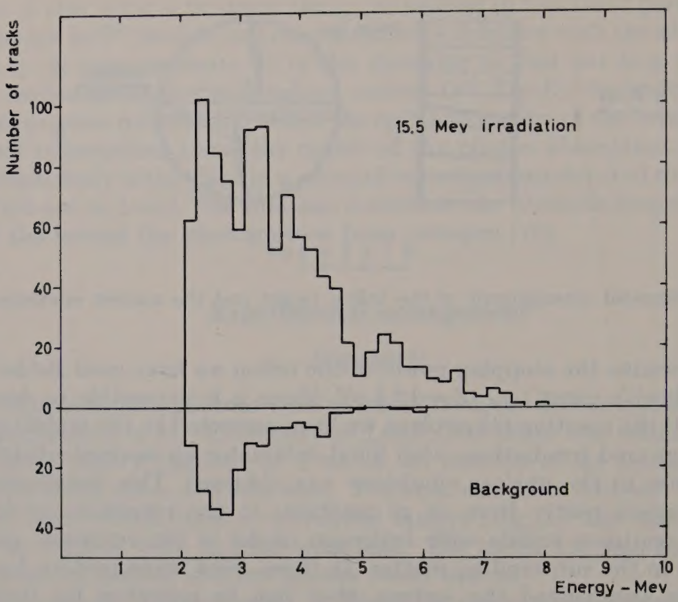

Fig. 2. The proton distribution from the 15.5 MeV irradiation. The background is shown downwards.

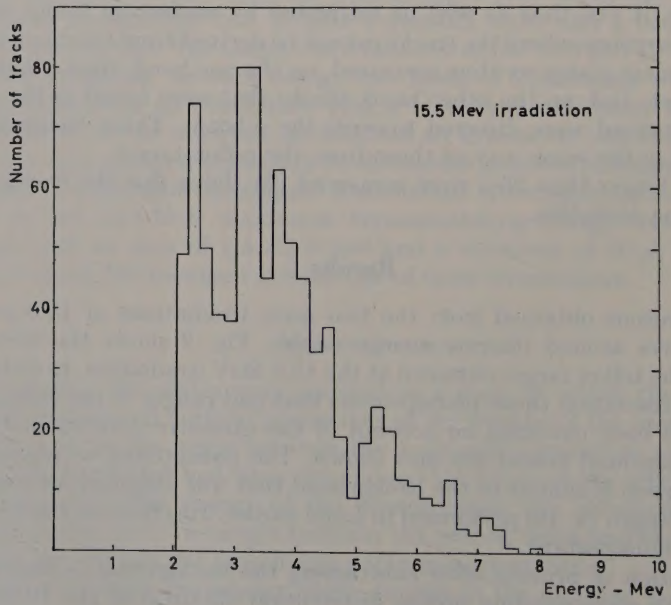

Fig. 3. The proton distribution from the 15.5 MeV irradiation after the background is subtracted.

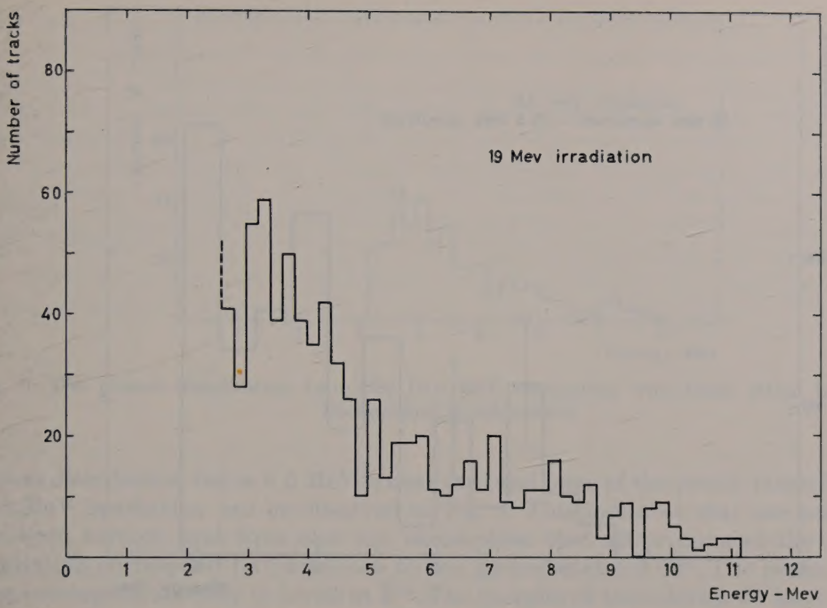

Fig. 4. The proton distribution from the 19 MeV irradiation after the background is subtracted.

The nuclear reactions that may take place in the teflon target in this experiment are:

(1) $F^{19}(\gamma, p)O^{18}$ $Q = -7.96$ MeV
(2) $F^{19}(\gamma, n)F^{18}$ $Q = -10.41$ MeV
(3) $F^{19}(\gamma, np)O^{17}$ $Q = -16.04$ MeV
(4) $F^{19}(\gamma, d)O^{17}$ $Q = -13.81$ MeV
(5) $F^{19}(\gamma, \alpha)N^{15}$ $Q = -3.99$ MeV
(6) $C^{12}(\gamma, p)B^{11}$ $Q = -15.96$ MeV
(7) $C^{12}(\gamma, \alpha)Be^{8}$ $Q = -7.38$ MeV

The photoneutrons are not recorded in this experiment. Since we only study track lengths longer than 25 μ, it is possible to separate proton tracks from α-tracks and thus photo-α-particles will not disturb our experiment.

Photodeuterons cannot, however, be distinguished from the photoprotons. As the threshold of $F^{19}(\gamma, d)$ is high the photodeuterons will not be recorded at the 15.5 MeV irradiation. On the other hand, the reaction might contribute in the lowest proton energy range at the 19 MeV irradiation. The cross-section of the (γ, d) reaction is not known, but presumably it is small compared to that of photoprotons. As both the $F^{19}(\gamma, np)$ and $C^{12}(\gamma, p)$ reactions can only contribute with protons below 3 MeV at the 19 MeV irradiation, only the proton distribution above 3 MeV has been marked in Fig. 4. The only nuclear reaction that has given rise to our proton distributions is thus F^{19} (γ, p).

In Fig. 3 (the 15.5 MeV irradiation) resolved peaks are observed at the proton energies 2.35, 3.25, 3.75, (4.55), and 5.35 MeV. In addition there are indications of new peaks at about 7 MeV. All these peaks are found in Fig. 4 (the 19 MeV irradiation), where we also observe other peaks both at energies above and below 7 MeV.

The experimental width of the energy peaks is due to the thickness of the teflon foil, uncertainty in the length measurements and straggling of the proton tracks.

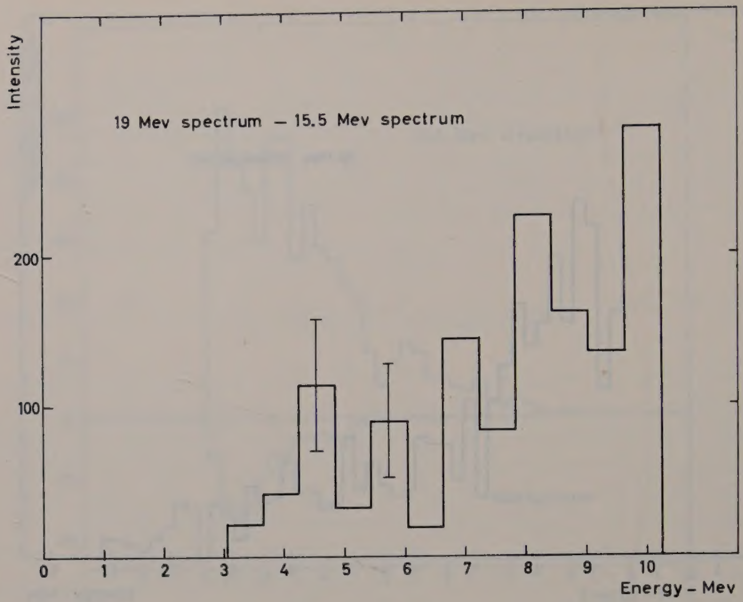

Fig. 5. The proton spectrum corresponding to photon absorption in the energy range 15.5.–19 MeV.

These errors can be estimated and give a total standard deviation of 0.2 MeV for a 3 MeV proton.

It is hard to analyse the observed proton distributions directly since they may contain peaks corresponding to transitions from F^{19} to both the ground state and the excited levels in O^{18}. Since the first excited levels in O^{18} are well separated and considerably higher than the ground state, it is possible to make an analysis of our proton distributions, if they are compared with one another. To be able to make this comparison we presume that all the protons in the 15.5 MeV irradiation correspond to transitions to the O^{18} ground state. Then we correct both proton distributions for the shape of the bremsstrahlung spectrum and normalize them to the same dose of X-rays. If the spectrum from the 15.5 MeV irradiation is then subtracted from the 19 MeV irradiation spectrum, one obtains a proton spectrum that corresponds to the photon absorption in the energy range 15.5–19 MeV. The normalizing could, of course, be carried out by measuring the dose with great accuracy, but in that case the geometry and scanning must be exactly the same in the two irradiations. These conditions are not entirely fulfilled. A better method of normalizing is to compare the number of protons in the two irradiations in a certain energy interval. The sharp proton peak at 3.25 MeV of the 15.5 MeV irradiation is also found in the 19 MeV irradiation. Since the width of this peak at the two irradiations is equal to the estimated width of a peak of protons from a sharp resonance, no extra protons corresponding to transitions to the excited levels in O^{18} can be assumed to have contributed to this peak. For this reason we have used this 3.25 MeV peak to normalize the two irradiation spectra. Fig. 5 shows the difference between the 19 and 15.5 MeV distributions after they have been corrected and normalized according to the above. In this figure two distinct peaks appear at the 4.5 and 5.8 MeV energies. As for the rest, the

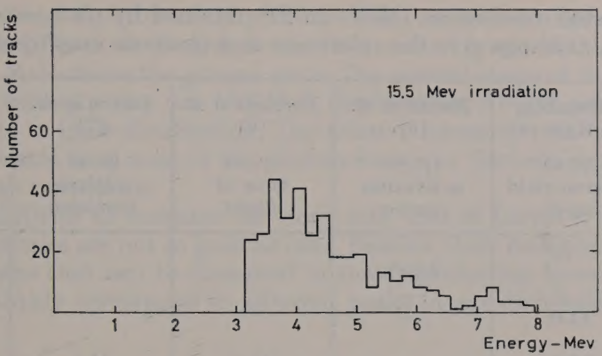

Fig. 6. The proton distribution from the 15.5 MeV irradiation with thick teflon target. The background is subtracted.

proton distribution below 6.5 MeV is near zero and none of the peaks, identified in the 15.5 MeV irradiation can be observed in Fig. 5. This indicates that our normalizing has been correct, and thus also our assumption that all protons at the 15.5 MeV irradiation correspond to transitions to the ground state of O^{18}. The peaks in Fig. 3 thus correspond directly to levels in F^{19}. The energies of these levels we have obtained by correcting the proton energies for the recoil energy of the O^{18} nucleus and by adding the threshold of the (γ, p) process. In this way we have obtained the following levels in F^{19} from the 15.5 MeV irradiation: 10.4, 11.4, 11.9, (12.8), and 13.6 MeV.

The photon absorption between 15.5 and 19 MeV can also be interpreted now. In Fig. 4 the peaks in the higher energy range are observed at 7.0, 8.1, and above 9 MeV. From (γ, n) measurements [3] we know that the giant resonance starts at 15 MeV. It is then natural to suppose that the above-mentioned peaks correspond to the ground-state transitions from levels in F^{19} that contribute to the giant resonance. Our peaks thus correspond to levels in F^{19} at 15.4, 16.5, and above 17.5 MeV. These levels are also de-excited through excited levels in O^{18}, which is seen in Fig. 5, where the proton peaks at 4.5 and 5.9 MeV correspond to such transitions.

The further irradiation at 15.5 MeV that was carried out to investigate the angular distribution of the protons also gives an energy distribution of the protons (Fig. 6). Since the teflon target is four times thicker, the energy correction will be so large that no discrete peaks can be expected, but the general shape of the distribution supports the earlier result. The 7 MeV peak can be observed especially in the higher energy range.

Comparison of the (γ, n) and (γ, p) reactions

The fine structure of the energy distribution of the photoprotons in this investigation should be compared with the observed fine structure of corresponding (γ, n) and (γ, p) reactions. Taylor *et al.* [3] have studied breaks in the (γ, n) activation curve, and Goldemberg and Katz [4] have investigated changes in the slope of the neutron-yield curve. Also Bendel *et al.* [5] have studied the activation curve in the neighbourhood of the threshold.

We can also compare this investigation with a recent work of Bertozzi *et al.* [6], who have studied the energy distribution of photoneutrons by time of flight technique.

Table 1. The reported resonances (MeV) in F^{19} obtained by photo-excitation. The column headings give the references and methods employed.

Taylor *et al.* [3] (γ, n) activation curve	Goldemberg and Katz [4] (γ, n) neutron-yield curve	Bendel *et al.* [5] (γ, n) activation curve	Bertozzi *et al.* [6] (γ, n) time of flight	Lasich *et al.* [7] (γ, p) nuclear emulsion	Present work (γ, p) nuclear emulsion
		10.47			10.4
10.6		—			—
10.9	11.0	—			—
11.2					—
11.5	11.5		11.5	11.1	11.4
11.9	11.9		12.0	12.0	11.9
12.2	—		12.2		
			13.0		(12.8)
	—		13.5	13.2	13.6
			14.4		
15.3	15.3		15.8		15.4
					16.5
					(18.1)

A (γ, p) investigation using the method applied in the present study has been carried out by Lasich *et al.* [7]. Although they were not able to identify a fine structure, one can, however, discern in their proton spectrum some of the peaks observed in our proton distribution. The results of the above-mentioned works are compared with the results of the present investigation in Table 1.

Bendel's *et al.* investigation of the (γ, n) activation curve from the threshold up to 11.1 MeV is the most accurate of those mentioned. They have observed a very sharp break at 10.47 MeV. Neither Taylor nor Goldemberg and Katz observed this break, probably owing to the fact that it lies immediately above the threshold for the (γ, n) reaction. This resonance is easily distinguished in our proton distribution (Fig. 3), corresponding to an excitation energy of 10.4 MeV. Bendel has, on the other hand, not observed any sharp breaks at 10.6 and 10.9 MeV; vague breaks may possibly exist but it is difficult to determine their positions. This does not confirm the results of Taylor and Goldemberg and Katz. Like Bendel, we have not observed any well-resolved proton peaks in this energy range.

The strongly marked breaks at 11.5, 11.9, and 15.3 MeV observed by Taylor and Goldemberg and Katz are seen in our proton distributions as distinct peaks at the excitation energies 11.4, 11.9, and 15.4 MeV. The energy resolution in our experiment is not sufficient for us to draw any conclusions regarding a probable level at 12.2 MeV. This has been observed by Taylor, but Goldemberg and Katz have not been able to reproduce this. In both our proton distributions we have, however, observed a distinct peak corresponding to an excitation energy of 13.6 MeV. This peak must be due to the transition of the photoprotons to the ground state of O^{18}, since it is not found in Fig. 5, where it would otherwise appear as an extremely strong peak. In this energy range Goldemberg and Katz have published an accurate yield curve, in which they have not been able to observe any break. This discrepancy is difficult to explain. Our 16.5 MeV level has not earlier been observed.

Bertozzi's energy distribution of photoneutrons contains a number of well-resolved peaks but it is difficult to analyse as the first excited levels of the daughter nucleus F^{18} are only 1 MeV above the ground state. The general shape of the energy spectrum is, however, strikingly like our 15.5 MeV distribution. All our peaks correspond directly to peaks in their distribution. The relative intensity ratio is also of the same size. This indicates that most of the photoneutrons in Bertozzi's experiment are due to ground-state transitions.

It is more difficult to compare our work with that of Lasich *et al.* Their resolving power and statistics are not so good as ours. Besides, their background seems disturbing. Those peaks that can be discerned in their distribution have been given in the table and probably correspond to adjacent peaks in our distributions.

The de-excitation process

From Fig. 5, which shows the photon absorption in the energy range 15.5–19 MeV, one can see how the excited F^{19} nucleus decays. The protons with energies below 6.5 MeV must be due to transitions to excited levels in O^{18}. The first levels of the O^{18} nucleus lie at 1.98, 3.55, and 3.93 MeV [13]. Since O^{18} is an even-even nucleus the ground state is 0^+. The first excited level is 2^+ and the second 4^+. The spin and parity of the third level are so far unknown. In spite of considerable statistical errors in Fig. 5, two peaks at 4.5 and 5.8 MeV are observed. These are naturally explained, if they are assumed to be transitions from levels in the giant resonance in F^{19} to the 3.93 MeV level in O^{18}. Then the 4.5 MeV peak would correspond to the 16.5 MeV level, which we have already observed, since it is also de-excited to the ground state in O^{18}. In analogy with this the 5.9 MeV peak should correspond to a level at 18 MeV. A trace of this peak is seen in Fig. 4. The peak at 7.0 MeV probably corresponds to the excited level at 15.4 MeV in F^{19} and arises when this level is de-excited to the ground state in O^{18}. Its appearance in Fig. 5 is explained by the fact that the maximum bremsstrahlung energy at our first main irradiation has been so near this value that the number of photoprotons in Fig. 3 from this level must be fairly uncertain.

If it is instead assumed that the de-excitation takes place to the 2^+ level at 1.98 MeV in O^{18}, it will be difficult to interpret the experimental result. With this assumption the photoprotons with energies below 6.5 MeV will have too low energy to arise from excited levels of the F^{19} nucleus in the energy range 15.5–19 MeV.

A de-excitation to the 4^+ level in the O^{18} nucleus is hard to imagine. The photoabsorption is assumed to be E1, and hence the excited levels in F^{19} must be $1/2^-$ or $3/2^-$. Should they be de-excited to 4^+, this must be done by *f*-wave protons, which means a high centrifugal barrier.

The giant resonance arises when a nucleon in the core is excited by photo-absorption. This nucleon can either form a compound nucleus or it can be thrown out directly without sharing its energy with the other nucleons, leaving the daughter nucleus with a hole in the core. This experiment indicates that the 3.96 MeV level in O^{18} is an excited level with a hole in the *p*-shell. On this account it should have a spin of 0, 1 or 2 and negative parity.

The first two levels in O^{18} with 2^+ and 4^+ probably have no rotational character, for in such a case the ratio between their energies would be more than twice the present value. The level 2^+ is then probably of vibrational character, which may explain the fact that we have not observed any transitions to this level.

The γ-absorption

After interpreting the peaks in our proton distributions it is possible to calculate the cross-section curve for the (γ, p) reaction in fluorine. This is shown in Fig. 7. The scale for the cross-section curve is given in arbitrary units, as our experiment does not provide information on the absolute cross-section. Fig. 7 shows also the levels in F^{19} obtained in this investigation. The way in which these are de-excited to O^{18} by proton emission has been marked. The branching ratios from the higher levels in F^{19} to the O^{18} levels has been estimated from Fig. 5. It is interesting to compare the cross-section curves of the (γ, p) and (γ, n) reactions. Because of this, the cross-section curve of the (γ, n) reaction in fluorine from Taylor *et al.* [3] has been drawn in the figure. This is given in absolute units. From the figure it is seen that the general shapes of the curves agree. We have already shown that the fine structure in the (γ, n) absorption agrees well with that in our (γ, p) results. Only if the daughter nuclei of the two reactions are mirror nuclei can one conclude that the cross-sections of the two reactions are alike. This is not the case in F^{19}. The total photon-absorption curve,

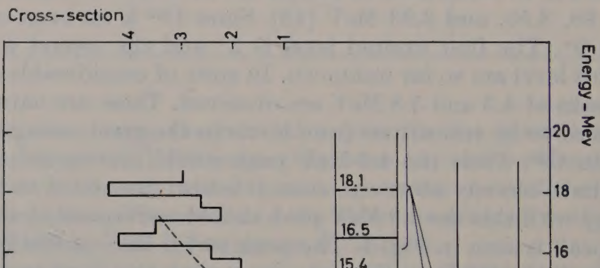

Fig. 7. The level scheme for the photo-disintegration of F^{19}. The histogram to the left gives the cross-section for (γ, p) in arbitrary units. The dotted curve shows the (γ, n) cross-section from [3] in millibarns. The numbers for some of the transitions to O^{18} denote the relative branching ratios in per cent.

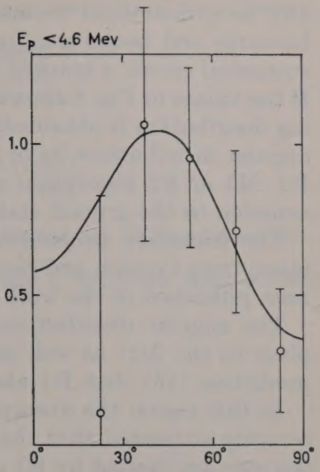

Fig. 8. The angular distribution of the protons with energies less than 4.6 MeV from the 15.5 MeV irradiation with thick teflon target.

however, must have a pronounced peak around 12 MeV, since both the (γ, n) and (γ, p) curves here have maxima. These two processes are the only ones, excepting the (γ, γ) reaction, that contribute to the absorption in this energy range.

The absorption curve then rises strongly when we enter the giant resonance and reaches its highest value at 22 MeV [2]. The width of the giant resonance is great [14], which should be expected, as the F^{19} nucleus is strongly deformed. The pygmy resonance which has been observed at 12 MeV is not part of the giant resonance and should not be interpreted as the first of the two peaks into which the giant resonance of a strongly deformed nucleus is split. It is too small for this and the energy value is too low.

The angular distribution of the photoprotons from the pygmy resonance suggests the nature of the photo-absorption in this energy region. This is shown in Fig. 8 after a correction for the solid angle has been made. The distribution should theoretic-

Table 2. Theoretical angular distribution for proton transitions between states in the excited F^{19} nucleus (spin J_c) to the ground state of O^{18} nucleus (spin 0^+). The ground state of F^{19} is $1/2^+$. S denotes the channel spin and l the orbital angular momentum of the proton.

Type of photon absorption	J_c	l	S	Angular distribution
E 1	$1/2^-$	1	1/2	Isotropic
E 1	$3/2^-$	1	1/2	$1+\frac{3}{2}\sin\theta$
M 1	$1/2^+$	0	1/2	Isotropic
M 1	$3/2^+$	2	1/2	$1+\frac{3}{2}\sin^2\theta$
E 2	$3/2^+$	2	1/2	$1+\cos^2\theta$
E 2	$5/2^+$	2	1/2	$1+6\cos^2\theta - 5\cos^4\theta$

ally be symmetrical around 90°, which our experiment confirms. The distribution forwards and backwards has been added to improve the statistics. In spite of large statistical errors, a marked decrease towards higher angles is seen in the distribution. If the values in Fig. 8 are weighted and fitted by the least-squares method, the following distribution is obtained: $1 + 7 \cos^2 \theta - 6 \cos^4 \theta$. To confirm the above, the possible angular distributions have been calculated for the case when F^{19} is excited through E1, M1 or E2 absorption and the excited level has then been de-excited by proton emission to the ground state in O^{18}. LS-coupling has been presumed.

The transition probabilities to the $(2J + 1)$ states in the excited level has been taken from Condon and Shortley [15]. The result is shown in Table 2. This has earlier been published in the work by Lasich *et al.* [7].

The angular distribution obtained will be explained if E2 absorption has taken place to the $3/2^+$ as well as the $5/2^+$ level. This agrees with Blatt and Weisskopf's prediction [16] that E1 absorption is strongly suppressed below 15 MeV.

In this region the absorption should then go through M1 and E2. Fujii [17] has recently suggested that the pygmy resonance arises when the free nucleons outside the core are excited by E1 absorption. His estimations for fluorine give a sharp peak at 14 MeV. Fujii gives $6 + 5 \sin^2 \theta$ for the angular distribution of the photoneutrons. This angular distribution should under these assumptions be valid also for photoprotons. The fine structure in the pygmy resonance and our observed angular distribution of photoprotons cannot be explained according to Fujii's theory. Nor does the width and position of the resonance agree with this theory.

Conclusions

In this experiment we have observed the fine structure in the (γ, p) absorption in F^{19}. This fine structure corresponds to well-defined excited levels in F^{19}, which are presented in Table 1. Most of these levels have earlier been observed in the (γ, n) absorption curve, which demonstrates the close connection between the (γ, p) and (γ, n) reactions. The de-excitation by proton emission of the levels in F^{19} goes partly through excited levels in O^{18}. Our experiment suggests that the level in O^{18} at 3.93 MeV is a state with a hole in the core. The angular distribution of the photoprotons from the pygmy resonance at 12 MeV in fluorine suggests that E1 absorption in this region is strongly suppressed. Thus the pygmy resonance should not be supposed to arise from E1 absorption.

ACKNOWLEDGEMENT

The present investigation was suggested by Dr. S. A. E. Johansson to whom the authors are deeply indebted for many stimulating and valuable discussions. The authors are grateful to Mr. W. Stiefler for helping with measurements and calculations and to Mr. L. Hansson for skilful technical assistance.

REFERENCES

1. R. J. Horsley, R. N. H. Haslam, and H. E. Johns, Phys. Rev. *87*, 756 (1952).
2. G. A. Ferguson, J. Halpern, R. Nathans, and P. F. Yergin, Phys. Rev. *95*, 776 (1954).
3. J. G. V. Taylor, L. B. Robinson, and R. N. H. Haslam, Can. J. Phys. *32*, 238 (1954).
4. J. Goldemberg and L. Katz, Phys. Rev. *95*, 471 (1954).
5. W. L. Bendel, J. McElhinney, and R. A. Tobin, Phys. Rev. *111*, 1297 (1958).

6. W. BERTOZZI, S. KOWALSKI, F. PAOLINI, and C. SARGENT, Massachusetts Institute of Technology Progress Report, November 1, 1959, p. 81.
7. W. B. LASICH, E. G. MUIRHEAD, and G. G. SHUTE, Aust. J. Phys. *8*, 456 (1955).
8. S. A. E. JOHANSSON and B. FORKMAN, Phys. Rev. *99*, 1031 (1955).
9. S. A. E. JOHANSSON and B. FORKMAN, Ark. f. Fysik *12*, 359 (1957).
10. I. WAHLSTRÖM and B. FORKMAN, Ark. f. Fysik *18*, 83 (1960).
11. W. H. BARKAS, Nuovo Cimento *8*, 201 (1958).
12. M. S. LIVINGSTON and H. A. BETHE, Rev. Mod. Phys. *9*, 245 (1937).
13. F. AJZENBERG-SELOVE and T. LAURITSEN, Nucl. Phys. *11*, 1 (1959).
14. S. A. E. JOHANSSON, Ark. f. Fysik *13*, 331 (1958).
15. E. U. CONDON and G. H. SHORTLEY, The Theory of Atomic Spectra, p. 79 (Cambridge University Press 1953).
16. J. M. BLATT and V. F. WEISSKOPF, Theoretical Nuclear Physics, p. 651 (John Wiley & Sons, New York, 1952).
17. S. FUJII, Progr. Theor. Phys. *21*, 511 (1959).

Tryckt den 23 september 1960

Uppsala 1960. Almqvist & Wiksells Boktryckeri AB